SCIENCE CHINA Materials ARTICLES

mater.scichina.com link.springer.com

Published online 11 October 2019 | https://doi.org/10.1007/s40843-019-1174-3

*Sci China Mater* 2020, 63(1): 47–54

# Ambient stable $FAPbI_3$-based perovskite solar cells with a 2D-$EDAPbI_4$ thin capping layer

Ya-Han Wu[1], Yong Ding[1*], Xiao-Yan Liu[3], Xi-Hong Ding[1], Xue-Peng Liu[1], Xu Pan[2*] and Song-Yuan Dai[1,2*]

**ABSTRACT** **Two-dimensional (2D) lead halide perovskite materials are emerging as one of promising light-absorbing materials in perovskite solar cells (PSCs), which show outstanding stability and defect passivation. Unfortunately, the power conversion efficiency (PCE) of those stable 2D PSCs is still far behind that of 3D PSCs. Herein, we reported a simple *in-situ* growth technique for the ethylenediamine lead iodide ($EDAPbI_4$) layer on the top of formamidinium lead iodide ($FAPbI_3$) layer. The rationally designed layered architecture of 2D-3D perovskite film could improve the PCE of the PSCs. In addition, benefiting from the high moisture resistance and inhibited ion migration of $EDAPbI_4$ layer, the 2D-3D-based devices showed obviously enhanced long-term stability, keeping the initial PCE value for 200 h and 90% of its initial PCE even after 500 h.**

**Keywords:** $EDAPbI_4$, $FAPbI_3$, 2D-3D, perovskite solar cell, stability

## INTRODUCTION

Lead halide perovskite solar cells (PSCs) have attracted extensive attention due to their rapidly boosted performance, and certified maximum power conversion efficiency (PCE) has reached up to 24.2% [1,2]. Such an amazing development is due to high absorption coefficient, long balanced carrier diffusion length, and the advantages of easy solution of perovskite materials [3,4]. In recent years, two-dimensional (2D) perovskites are another branch of perovskite materials and have been widely used in PSCs, due to their unique structural characteristics. 2D perovskite films with long-chain organic cations show excellent tolerance to moist environment [5–11]. However, the 2D perovskite not only slows the charge transfer between perovskite layers but also reduces the electron collection efficiency of electron transport or hole transport layer [12]. The 2D perovskite-based PSCs always exhibit inferior performance than conventional 3D devices [13].

In a previous study, introducing 2D perovskite into 3D perovskite materials has been considered as a common method to improve the long-term stability of the PSC without sacrificing too much photovoltaic performance. Smith *et al.* [14] reported $(PEA)_2(MA)_2Pb_3I_{10}$ (PEA=$C_6H_5(CH_2)_2NH_3^+$, MA=$CH_3NH_3^+$)-based 2D perovskite material and obtained a PCE of 4.73% in 2014. Recently, Tsai *et al.* [15] reported an enhanced PCE of 12.52% using 2D $(CH_3(CH_2)_3NH_3)_2(CH_3NH_3)_2Pb_3I_{10}$ and $(CH_3(CH_2)_3NH_3)_2(CH_3NH_3)_3Pb_4I_{13}$ perovskite films, and the devices exhibited improved stability when subjected to light and humidity. In the 2D perovskite materials mentioned above, instead of methylammonium (MA) or formamidinium (FA), larger organic molecules were used to develop photovoltaics [16]. Compared with 3D perovskite, the layered 2D perovskite could provide more environmental stability due to the stronger van der Waals interaction between organic molecules and $PbI_6$. Moreover, the long chain organic ion was more hydrophobic than FA or MA ions, which was conducive to improving the stability against humidity [17]. More recently, the PSCs based on $(C_6H_5C_2H_4NH_3)_2(CH_3NH_3)_{n-1}Pb_nI_{3n+1}$ ($n$=60) have achieved a certified PCE of 15.3%, but the device stability was not so good because of the reduced content of 2D perovskite [18]. Therefore, for further practical application of PSCs, it is urgent to develop a simple and feasible method to balance the PCE and long-term stability of the devices.

[1] Beijing Key Laboratory of Novel Thin-Film Solar Cells, North China Electric Power University, Beijing 102206, China
[2] Key Laboratory of Photovolatic and Energy Conservation Materials, Institute of Applied Technology, Hefei Institutes of Physical Science, Chinese Academy of Sciences, Hefei 230031, China
[3] School of Economics and Management, North China Electric Power University, Beijing 102206, China
* Corresponding authors (emails: dingy@ncepu.edu.cn (Ding Y); xpan@rntek.cas.cn (Pan X); sydai@ncepu.edu.cn (Dai SY))

  

In this work, we introduced a simple method to fabricate a thin 2D ethylenediamine lead iodide ($EDAPbI_4$) layer on the top of 3D formamidinium lead iodide ($FAPbI_3$) layer for efficient and stable 2D-3D-based devices. It is noted that the device with 2D perovskite capping layer resulted in obviously enhanced open-circuit voltage ($V_{oc}$) and fill factor (FF). Most importantly, the 2D-3D-based devices exhibited significant long-term stability.

## RESULTS AND DISCUSSION

The deposition process of 2D-3D perovskite film is displayed in Fig. 1a, which is divided into four steps. Firstly, the FAI/$PbI_2$ precursor solution was spin-coated on the mesoporous layer and then antisolvent solution was dropped on the film. Subsequently, the film was annealed at 140°C for 30 min to obtain the $FAPbI_3$ perovskite film. Thirdly, the saturated ethanediaminedihydroiodide ($EDAI_2$) solution (Fig. S1) was spin-coated on the $FAPbI_3$ perovskite film to grow an additional 2D $EDAPbI_4$ film. Finally, the $EDAPbI_4$ capping layer was successfully obtained on the top of the $FAPbI_3$ film after annealing at 140°C for 10 min.

X-ray diffraction (XRD) patterns, photographs and ultraviolet-visible (UV-Vis) spectra of the 2D-3D heterojunction- and 2D/3D hybrid-structure (10:0, 8:2, 6:4, 4:6, 2:8, and 0:10, volume ratio) perovskite films were measured in Fig. 2 and Fig. S2 (the details on the 2D/3D films preparation were given in the supporting information). For the 2D film (2D/3D, 10:0), the characteristic peaks located at 8.7° and 9.3° indicated the formation of 2D $EDAPbI_4$ film. Moreover, an absorption at ~420 nm observed in the UV-Vis spectra indicated that the $EDAPbI_4$ was a wider band-gap material (Fig. S1) [19]. With the decrease of 2D content to 60%, the characteristic peaks of 2D perovskite disappeared completely [20], while the typical peak (13.8°) of 3D perovskite film was observed in Fig. 2a. However, it was noteworthy that the weak peaks corresponding to the 2D perovskite at 26.5° and 33.7° were observed at small angles in the diffraction, which also proved the existence of 2D materials in 2D-3D and 2D/3D (10:0, 8:2, 6:4, 4:6 and 2:8) films in Fig. 2b, c.

The morphological structure of the 3D and 2D-3D films were examined by scanning electron microscopy (SEM) and shown Fig. 3. Although the surface coverage of 3D film was complete, the grain boundaries, and pinholes were still observed in Fig. 3a. After $EDAI_2$ treatment, the morphology of 3D film has considerably changed. A uniform and pinhole-free 2D-3D film was found in Fig. 3b. Previous studies reported that the in-

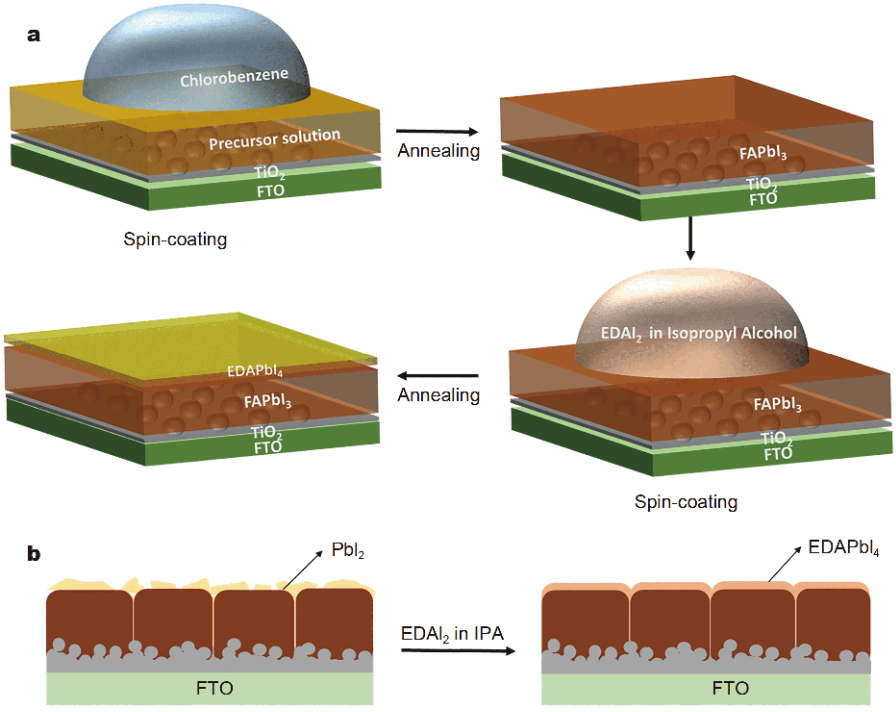


**Figure 1** (a) Illustration of the method for fabricating a 2D-3D perovskite film by spin-coating $EDAI_2$ in isopropyl alcohol (IPA) on the $FAPbI_3$ film; (b) proposed changes of cross-sectional structures of the 3D and the 2D-3D perovskite films.

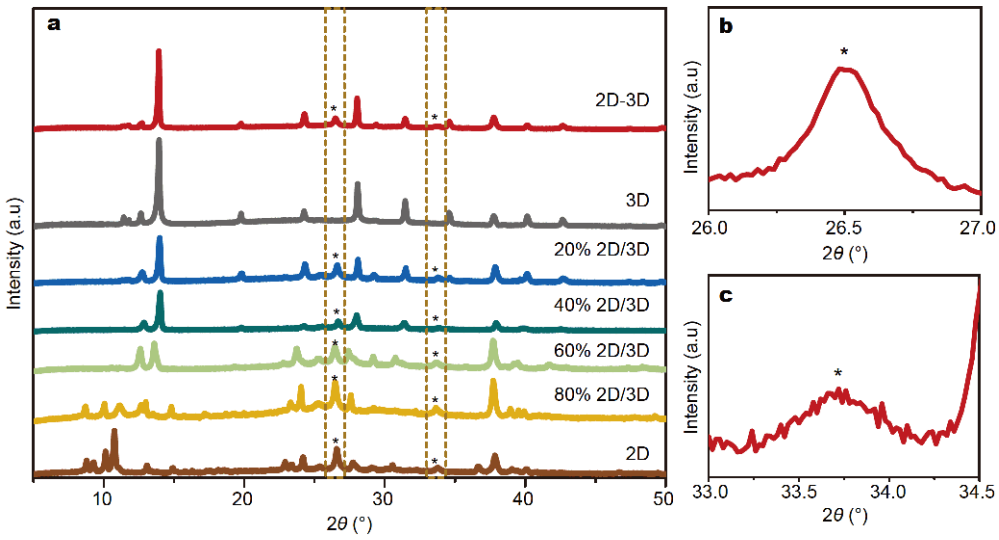


**Figure 2** (a) XRD patterns of 2D-3D and 2D/3D (10:0, 8:2, 6:4, 4:6, 2:8, and 0:10, volume ratio) perovskite films. XRD pattern of 2D-3D perovskite film at (b) 26.5° and (c) 33.7°.

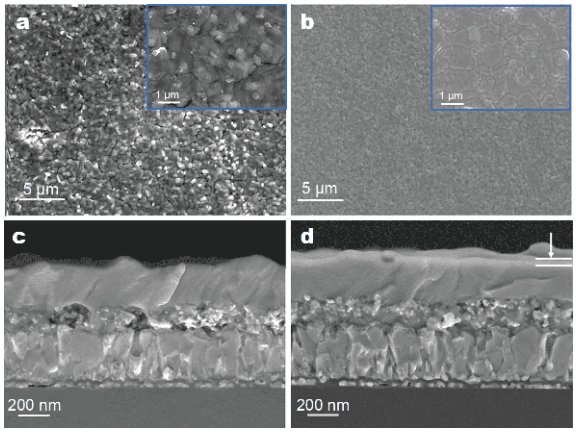


**Figure 3** (a, b) SEM top-view images and (c, d) the corresponding cross-sectional SEM images of 3D and 2D-3D perovskite films.

corporation of long chain alkyl-ammonium halides was beneficial to reducing the pinholes and passivating their surface [21–23]. Additionally, the $PbI_2$ particles on the 3D film were significantly reduced, which might be the result of the reaction between $EDAI_2$ solution and excessive $PbI_2$ on the 3D film surface (Fig. 1b). Meanwhile, the cross-sectional SEM image showed that the additional layer with a thicknesss of about 50 nm formed on the 3D perovskite layer, suggesting the formation of 2D perovskite layer in Fig. 3d.

X-ray photoelectron spectroscopy (XPS) was used to study the formation of 3D, 2D and 2D-3D perovskite films. As can be seen from Fig. 4a, the C–C (284.8 eV) and C–N (286.5 eV) bonds were detected in C 1s XPS spectrum of 3D-$FAPbI_3$ film, suggesting the existence of $FA^+$ cation [24]. In addition, the C=O bond at 288.3 eV emerged in $FAPbI_3$ film was due to the introduction of $H_2O$ and $O_2$ in the preparation process of $FAPbI_3$ [25,26]. In the N 1s peak (Fig. 4d), the bond of C–N at 400.4 eV and C=N at 402.3 eV came from the $C–NH_2$ and $C=NH_2^+$ of $FAPbI_3$ [24]. As a contrast, for the 2D film, the C–C and C–N bonds of 2D perovskite film at 284.3 and 286.5 eV increased significantly in Fig. 4b. It showed that the C–C and C–N bonds in 2D perovskite were more than those in 3D perovskite, verifying the presence of $EDA^{2+}$ ($NH_3^+C_2H_4NH_3^+$) cation. Notably, the disappearance of C=O band indicated the high stability of 2D perovskite film to $H_2O$ and $O_2$. The N 1s spectrum of 2D perovskite film has two peaks at 401.7 and 399.2 eV, which were consistent with the previously reported 2D $EDAPbI_4$ film in Fig. 4e [19]. According to the chemical structure in Fig. S3, the strong peak at 401.7 eV could be ascribed to the C–N of $EDA^{2+}$ and the other peak at 399.2 eV was due to N in the $–NH_2$ state. Finally, for the 2D-3D film, the typical peaks of $FAPbI_3$ and $EDAPbI_4$ films could be found in the C 1s and N 1s spectra in Fig. 4c, f, suggesting that 2D perovskite film has been successfully grown on 3D perovskite film. Meanwhile, the weakening of C=O in Fig. 4c revealed the effect of water-resistant of 2D perovskite layer and passivated ionic vacancies. Moreover, as shown in Fig. S4, compared with 3D perovskite film, the peak positions of Pb 4f and I 3f shifted slightly to the higher binding energy, which sug-

  

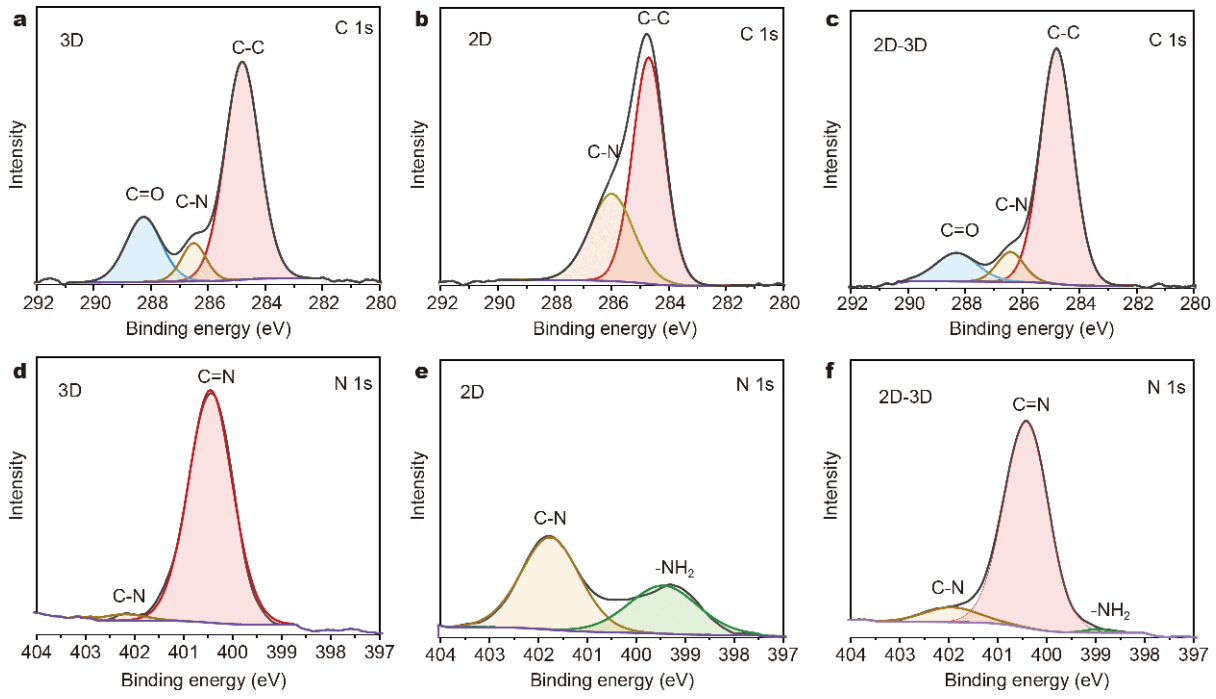


**Figure 4** XPS spectra of (a–c) C 1s, and (d–f) N 1s of 3D, 2D and 2D-3D perovskite films.

gested that the chemical environments of Pb and I in 2D-3D were different from those in 3D perovskite film [27].

The electrical properties of the device interface were investigated by using electrochemical impedance spectroscopy (EIS). In general, the first semicircle stands for the charge transfer. As shown in Fig. 5a, the first semicircle of the 3D based device was slightly lower than that of 2D-3D-based device, demonstrating that 3D-based device had a slightly larger charge transport resistance ($R_{ct}$) than 2D-3D-based devices. On the other hand, the second semicircle stands for the charge recombination at the interface between titanium dioxide and perovskite [28–31]. The semicircle of the device based on 2D-3D film was larger than that of device based on 3D film, which showed that the charge recombination could be remarkably suppressed due to the reduced defect density.

To confirm the effect of 2D film, photoluminescence (PL) and time resolved PL (TRPL) were carried out to probe to the dynamics of recombination.

The TRPL and PL of 3D and 2D-3D perovskite films on the glass were measured in Fig. 5b, c. 2D-3D film had a stronger PL intensity compared with 3D film. The

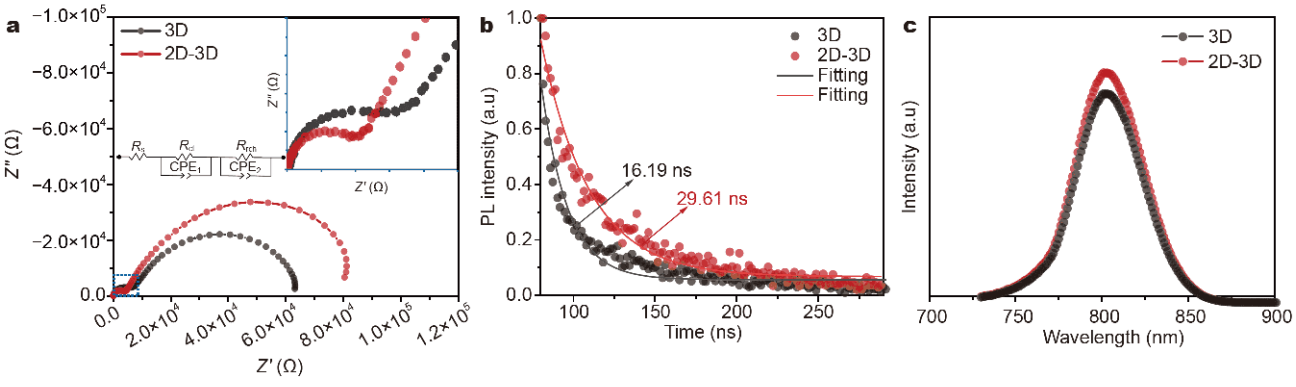


**Figure 5** (a) Nyquist plots of the devices based on 3D and 2D-3D perovskite films (under constant illumination conditions at the bias of 30 mV). (b) TRPL and (c) PL spectra for the 3D and 2D-3D perovskite films on glass.

increased PL intensity could be attributed to the reduced surface traps by $EDAI_2$ treatment. By fitting single index model for the 3D and 2D-3D films, PL lifetimes of the 3D and 2D-3D films were calculated to be 16.19 and 29.61 ns, respectively. This phenomenon displayed improved perovskite film and reduced grain boundaries and defects after $EDAI_2$ treatment.

To examine the photoelectric properties, the devices were fabricated by using 3D and 2D-3D perovskite films. The device based on 2D-3D film showed a PCE of 17.96% under a reverse scan and 16.88% under a forward scan (Fig. 6a). The steady-state photocurrent and output power of the device based on 2D-3D film were measured for 300 s at the bias of 0.9 V. A steady photocurrent of 19.05 mA $cm^{-2}$ and corresponding PCE of 17.13% could be yielded in Fig. 6d. However, the optimal PCE of the device based on 3D reached 16.23% and 13.08%, respectively, under a reverse and forward scan (Fig. 6b). The FF and $V_{oc}$ of the device based on 2D-3D were significantly improved, indicating the charge recombination could be remarkably suppressed due to the reduced defect density [32]. Moreover, the photon-to-current efficiency

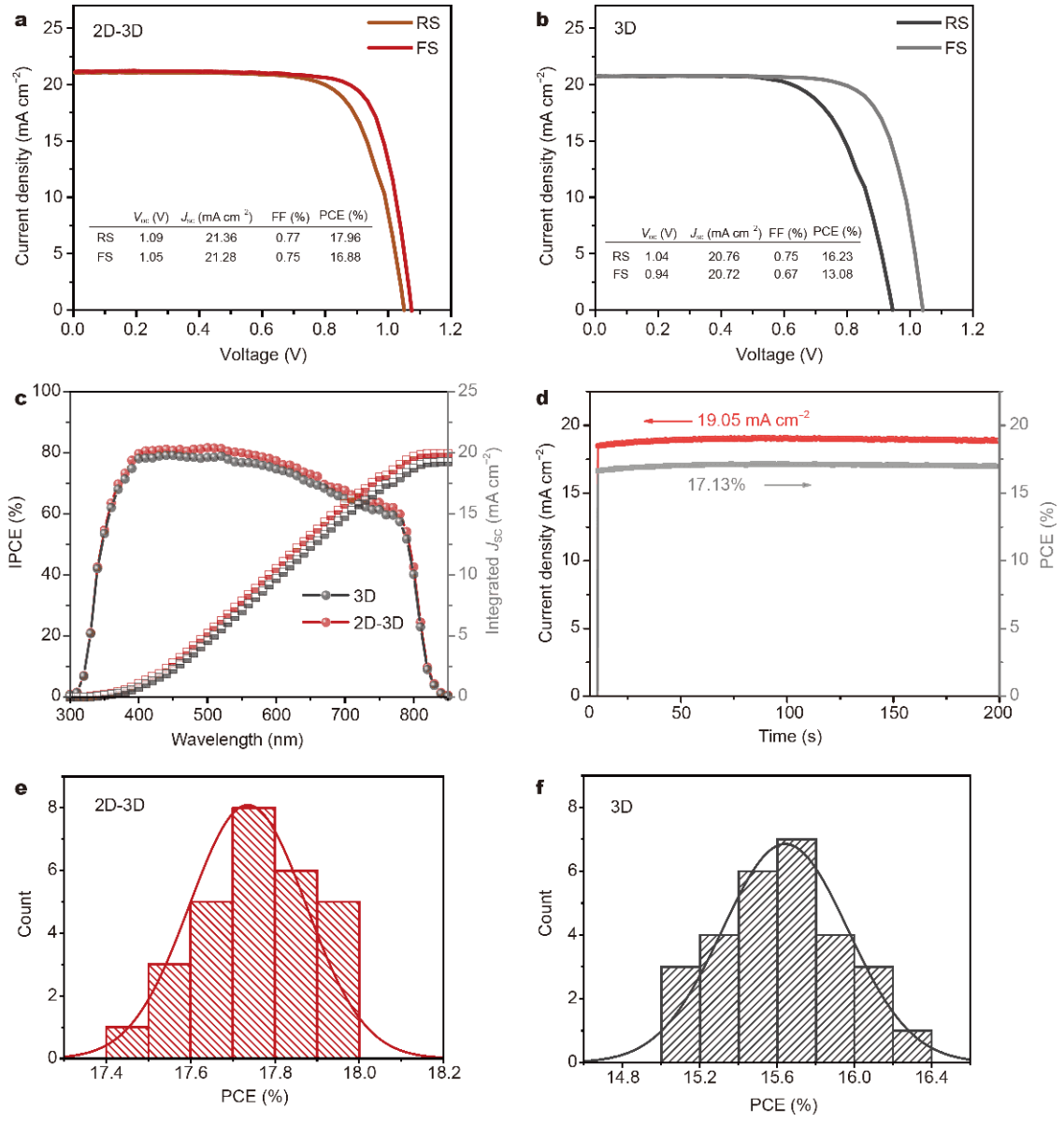


**Figure 6** *J-V* curves of the devices based on (a) 2D-3D and (b) 3D. (c) IPCE of the devices based on 3D and 2D-3D. (d) Stable current output at maximum point of the device based on 2D-3D. Histograms of PSCs efficiency of the devices based on (e) 2D-3D and (f) 3D.

  

(IPCE) curve and the integrated short circuit current density ($J_{sc}$) value of the device based on 2D-3D film are shown in Fig. 6c. A slightly increase of IPCE value and the integrated $J_{sc}$ might be attributed to the improvement of perovskite film quality. The statistical distribution of PCE based on 28 devices suggested the reliability and repeatability of the devices (Fig. 6e, f).

To evaluate whether the 2D capping layer had a positive effect on the long-term stability of the devices, the devices were stored in an ambient condition with 30% relative humidity (RH) and 25°C for 200 h in dark. We monitored the changes of XRD patterns of the fresh and aged films. As shown in Fig. 7a, the peaks of $PbI_2$, δ-$FAPbI_3$ and α-$FAPbI_3$ at 12.9°, 11.8° and 13.8° were observed in fresh 3D perovskite film, which showed the instability of α-$FAPbI_3$ during preparation process. However, in 2D-3D film, the peaks of $PbI_2$ weaken after $EDAI_2$ treatment, which indicated that the reaction between $PbI_2$ and $EDAI_2$ occurred. After aging for 200 h, the reduced intensity of α-$FAPbI_3$ characteristic peak and the increased intensity of $PbI_2$ and δ-$FAPbI_3$ characteristic peaks demonstrated that the degradation was obvious in 3D-$FAPbI_3$ film [33,34]. However, the peaks of $PbI_2$ (12.9°), δ-$FAPbI_3$ (11.8°) and α-$FAPbI_3$ (13.8°) did not change significantly after aging for 200 h in 2D-3D film. Photographs of the films of 3D, 2D-3D, 3D-200 h and 2D-3D-200 h were inserted into Fig. 7a, respectively. After aging for 200 h, the color of 3D film has obviously changed from black to yellow. Compared with 3D film, 2D-3D film remained black after aging for 200 h, which

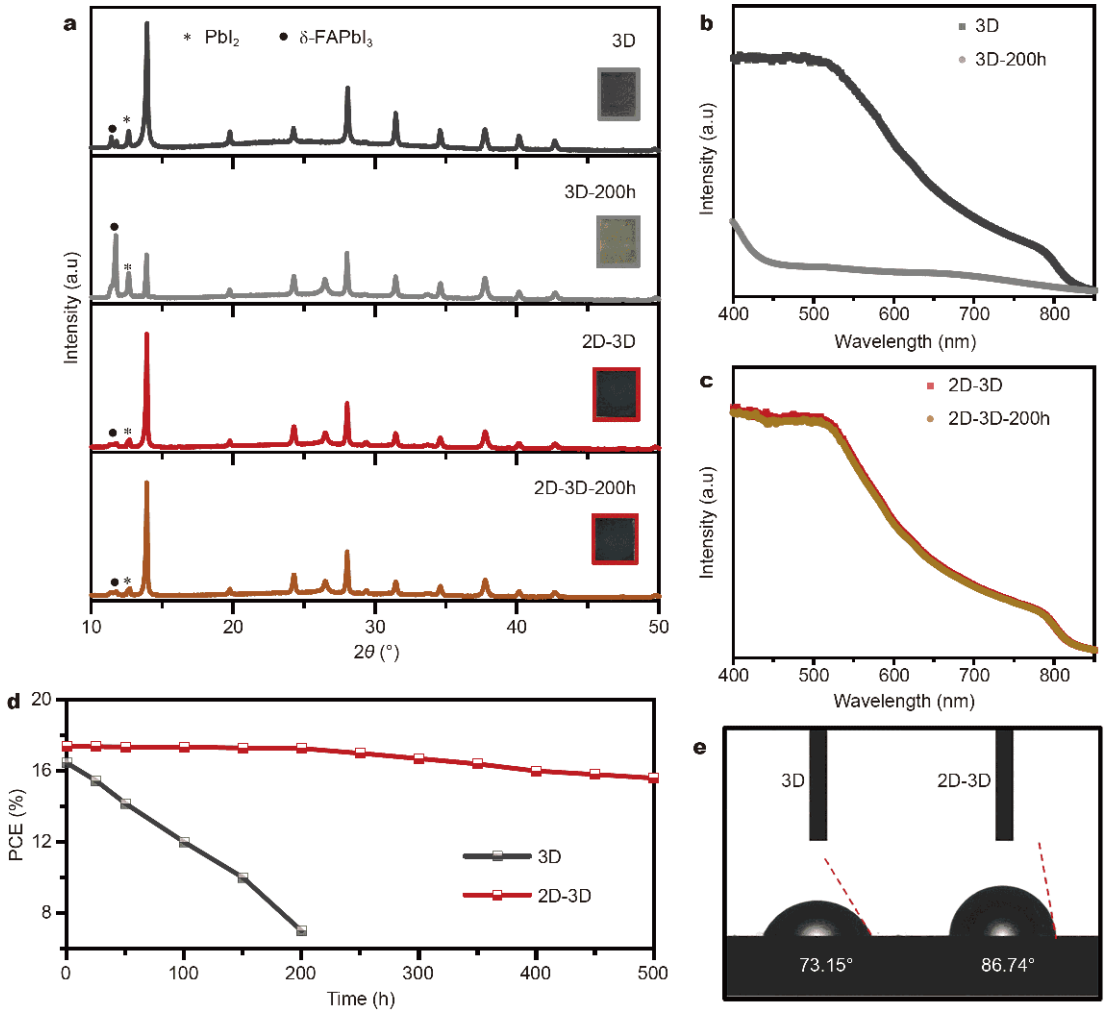


**Figure 7** (a) XRD patterns, photographs of 3D and 2D-3D films with and without aging for 200 h. UV-Vis spectra of (b) 3D films with and without aging for 200 h and (c) 2D-3D films with and without aging for 200 h. (d) Stability of devices based on 3D and 2D-3D. (e) Contact-angle measurements of water droplet on 3D and 2D-3D films. The devices were stored at an ambient condition with 30% RH at 25°C in dark.

also suggested that 2D films grown on 3D film had high moisture resistance. Furthermore, as shown in Fig. 7b, the absorbance of 3D film was significantly reduced after aging for 200 h. On the contrary, the absorption spectrum of 2D-3D film was almost unchanged after aging for 200 h. Fig. 7e displays the photographs of contact angles for 3D and 2D-3D films, demonstrating the enhancement of humidity resistance induced by 2D film, which helps to improve the stability of the film. In addition, the long-term stability has always been an urgent requirement for PSCs. The stability of the devices based on 3D and 2D-3D films was tested under 30% RH at 25°C. The PCE value of the device based on 3D gradually reduced to nearly zero with 200 h. In the meantime, the device based on 2D-3D film maintained the initial PCE value for 200 h, even after 500 h, it still maintained 90% of its initial PCE. It proved that the device based on 2D-3D film showed the excellent moisture stability, as illustrated in Fig. 7d.

## CONCLUSIONS

In conclusion, we developed a simple deposition method to simultaneously enhance stability and PCE of 3D-based device *via* forming $EDAPbI_4$ layer on the top of $FAPbI_3$ film. Such 2D capping layer could effectively suppress the charge recombination in 2D-3D PSCs, thus achieving higher PCE. At last, the 2D-3D-based device showed a PCE of 17.96%, which was higher than the 3D-based device. Benefiting from the high moisture resistance of the $EDAPbI_4$ film, the 2D-3D-based devices demonstrated remarkably enhanced long-term stability, keeping the initial PCE value for 200 h and maintaining 90% of its initial PCE even after 500 h in a constant temperature and humidity chamber with 30% RH and 25°C .

**Received 6 July 2019; accepted 29 August 2019; published online 11 October 2019**


1 Yang WS, Park BW, Jung EH, *et al.* Iodide management in formamidinium-lead-halide-based perovskite layers for efficient solar cells. Science, 2017, 356: 1376–1379
2 Best Research Cell Efficiencies. https://www.nrel.gov/pv/assets/pdfs/best-research-cell-efficiencies.20190802.pdf
3 Chen W, Wu Y, Yue Y, *et al.* Efficient and stable large-area perovskite solar cells with inorganic charge extraction layers. Science, 2015, 350: 944–948
4 Wu Y, Yang X, Chen W, *et al.* Perovskite solar cells with 18.21% efficiency and area over 1 $cm^2$ fabricated by heterojunction engineering. Nat Energy, 2016, 1: 16148
5 Cohen BE, Wierzbowska M, Etgar L. High efficiency and high open circuit voltage in quasi 2D perovskite based solar cells. Adv Funct Mater, 2017, 27: 1604733
6 Stoumpos CC, Cao DH, Clark DJ, *et al.* Ruddlesden-popper hybrid lead iodide perovskite 2D homologous semiconductors. Chem Mater, 2016, 28: 2852–2867
7 Zhao Z, Yin Z, Chen H, *et al.* High-performance, air-stable field-effect transistors based on heteroatom-substituted naphthalene-diimide-benzothiadiazole copolymers exhibiting ultrahigh electron mobility up to 8.5 cm $V^{-1}$ $s^{-1}$. Adv Mater, 2017, 29: 1602410
8 Zhang X, Munir R, Xu Z, *et al.* Phase transition control for high performance ruddlesden-popper perovskite solar cells. Adv Mater, 2018, 30: 1707166
9 Zhang Y, Wang P, Tang MC, *et al.* Dynamical transformation of two-dimensional perovskites with alternating cations in the interlayer space for high-performance photovoltaics. J Am Chem Soc, 2019, 141: 2684–2694
10 Zhu X, Xu Z, Zuo S, *et al.* Vapor-fumigation for record efficiency two-dimensional perovskite solar cells with superior stability. Energy Environ Sci, 2018, 11: 3349–3357
11 Cheng P, Wang P, Xu Z, *et al.* Ligand-size related dimensionality control in metal halide perovskites. ACS Energy Lett, 2019, 4: 1830–1838
12 Zhang T, Xie L, Chen L, *et al. In situ* fabrication of highly luminescent bifunctional amino acid crosslinked 2D/3D $NH_3C_4H_9COO(CH_3NH_3PbBr_3)_n$ perovskite Films. Adv Funct Mater, 2017, 27: 1603568
13 Cao DH, Stoumpos CC, Farha OK, *et al.* 2D homologous perovskites as light-absorbing materials for solar cell applications. J Am Chem Soc, 2015, 137: 7843–7850
14 Smith IC, Hoke ET, Solis-Ibarra D, *et al.* A layered hybrid perovskite solar-cell absorber with enhanced moisture stability. Angew Chem Int Ed, 2014, 53: 11232–11235
15 Tsai H, Nie W, Blancon JC, *et al.* High-efficiency two-dimensional Ruddlesden-Popper perovskite solar cells. Nature, 2016, 536: 312–316
16 Zhang X, Ren X, Liu B, *et al.* Stable high efficiency two-dimensional perovskite solar cells *via* cesium doping. Energy Environ Sci, 2017, 10: 2095–2102
17 Lermer C, Birkhold ST, Moudrakovski IL, *et al.* Toward fluorinated spacers for MAPI-Derived hybrid perovskites: synthesis, characterization, and phase transitions of $(FC_2H_4NH_3)_2PbCl_4$. Chem Mater, 2016, 28: 6560–6566
18 Quan LN, Yuan M, Comin R, *et al.* Ligand-stabilized reduced-dimensionality perovskites. J Am Chem Soc, 2016, 138: 2649–2655
19 Zhang T, Dar MI, Li G, *et al.* Bication lead iodide 2D perovskite component to stabilize inorganic α-$CsPbI_3$ perovskite phase for high-efficiency solar cells. Sci Adv, 2017, 3: e1700841
20 Jokar E, Chien CH, Fathi A, *et al.* Slow surface passivation and crystal relaxation with additives to improve device performance and durability for tin-based perovskite solar cells. Energy Environ Sci, 2018, 11: 2353–2362
21 Li G, Zhang T, Guo N, *et al.* Ion-exchange-induced 2D-3D conversion of $HMA_{1-x}FA_xPbI_3Cl$ perovskite into a high-quality $MA_{1-x}FA_xPbI_3$ perovskite. Angew Chem Int Ed, 2016, 55: 13460–13464
22 Cho KT, Paek S, Grancini G, *et al.* Highly efficient perovskite solar cells with a compositionally engineered perovskite/hole transporting material interface. Energy Environ Sci, 2017, 10: 621–627
23 Xiao Z, Bi C, Shao Y, *et al.* Efficient, high yield perovskite photovoltaic devices grown by interdiffusion of solution-processed precursor stacking layers. Energy Environ Sci, 2014, 7: 2619–2623
24 Chen P, Bai Y, Wang S, *et al. In situ* growth of 2D perovskite capping layer for stable and efficient perovskite solar cells. Adv Funct Mater, 2018, 28: 1706923


  

25 Bryant D, Aristidou N, Pont S, *et al.* Light and oxygen induced degradation limits the operational stability of methylammonium lead triiodide perovskite solar cells. Energy Environ Sci, 2016, 9: 1655–1660
26 Aristidou N, Eames C, Sanchez-Molina I, *et al.* Fast oxygen diffusion and iodide defects mediate oxygen-induced degradation of perovskite solar cells. Nat Commun, 2017, 8: 15218
27 Hu Y, Qiu T, Bai F, *et al.* Highly efficient and stable solar cells with 2D $MA_3Bi_2I_9$/3D $MAPbI_3$ heterostructured perovskites. Adv Energy Mater, 2018, 8: 1703620
28 Wu Y, Ding X, Shi X, *et al.* Highly efficient infrared light-converting perovskite solar cells: direct electron injection from $NaYF_4$:$Yb^{3+}$, $Er^{3+}$ to the $TiO_2$. ACS Sustain Chem Eng, 2018, 6: 14004–14009
29 Liu C, Yang Y, Ding Y, *et al.* High-efficiency and UV-stable planar perovskite solar cells using a low-temperature, solution-processed electron-transport layer. ChemSusChem, 2018, 11: 1232–1237
30 Lyu M, Yun JH, Cai M, *et al.* Organic-inorganic bismuth (III)-based material: a lead-free, air-stable and solution-processable light-absorber beyond organolead perovskites. Nano Res, 2016, 9: 692–702
31 Zheng H, Dai S, Zhou K, *et al.* New-type highly stable 2D/3D perovskite materials: the effect of introducing ammonium cation on performance of perovskite solar cells. Sci China Mater, 2019, 62: 508–518
32 Ma C, Shen D, Qing J, *et al.* Effects of small polar molecules ($MA^+$ and $H_2O$) on degradation processes of perovskite solar cells. ACS Appl Mater Interfaces, 2017, 9: 14960–14966
33 Wang Z, Zhou Y, Pang S, *et al.* Additive-modulated evolution of $HC(NH_2)_2PbI_3$ black polymorph for mesoscopic perovskite solar cells. Chem Mater, 2015, 27: 7149–7155
34 Ding X, Ren Y, Wu Y, *et al.* Sequential deposition method fabricating carbon based fully-inorganic perovskite solar cells. Sci China Mater, 2018, 61: 73–79


**Acknowledgements** This work was supported by the National Key Research and Development Program of China (2016YFA0202400), the 111 Project (B16016), the National Natural Science Foundation of China (51572080, 51702096 and U1705256), the Fundamental Research Funds for the Central Universities (2018ZD07, 2017MS021 and 2019MS027), and the Double Top Construction Program of North China Electric Power University (XM1805314).

**Author contributions** Wu YH prepared the perovskite films, fabricated the solar cell devices and wrote this manuscript. Pan X and Ding Y directly guided this research including the designing, modifying and optimizing work related to this manuscript. Dai SY supervised the projects and carefully reviewed and modified this manuscript. Liu XY, Ding XH and Liu XP performed the characterization. All authors contributed to the general discussion about this work.

**Conflict of interest** The authors declare that they have no conflict of interest.

**Supplementary information** Experimental details and supporting data are available in the online version of the paper.

**Ya-Han Wu** received her BSc degree from Inner Mongolia Normal University in 2011 and MSc degree from Inner Mongolia University in 2014, respectively. She is now a PhD candidate of the North China Electric Power University under the supervision of Profs. Xu Pan and Song-Yuan Dai. Her research interests mainly focus on perovskite solar cells.

**Yong Ding** received his PhD from Hefei Institutes of Physical Science, Chinese Academy of Sciences (CAS) in 2016, and became a lecturer in North China Electric Power University (NCEPU). His research interests are focused on the 2D perovskite-based photoelectric devices, including perovskite solar cells and light-emitting diodes.

**Xu Pan** received his PhD degree from the Chinese Academy of Sciences in 2007. He joined Hefei Institutes of Physical Science, CAS and was promoted to full professor in 2013. Now his research interest focuses on the new generation solar cells, including dye-sensitized solar cells and perovskite solar cells, etc.

**Song-Yuan Dai** is a professor of the School of Renewable Energy, North China Electric Power University. He obtained his BSc degree in physics from Anhui Normal University in 1987, and MSc and PhD degrees in plasma physics from the Institute of Plasma Physics, CAS in 1991 and 2001, respectively. His research interest mainly focuses on next-generation solar cells including dye-sensitized solar cells, quantum dot solar cells, perovskite solar cells, etc.

## 具有2D-$EDAPbI_4$薄覆盖层的环境稳定的$FAPbI_3$基钙钛矿太阳能电池

吴雅罕[1], 丁勇[1*], 刘晓燕[3], 丁希宏[1], 刘雪鹏[1], 潘旭[2*], 戴松元[1,2*]

**摘要** 二维(2D)卤化铅钙钛矿材料是钙钛矿太阳能电池(PSC)中最有前途的吸光材料之一, 具有优异的稳定性和缺陷钝化作用. 然而, 这些稳定的二维PSC的转换效率仍远远落后于三维钙钛矿电池. 在本文中我们通过原位生长的方法将2D EDAPbI$_4$层成功制备在3D FAPbI$_3$层表面。这种合理设计的2D-3D钙钛矿薄膜分层结构可以明显提高电池的效率. 另外, 由于EDAPbI$_4$层的高抗湿性和抑制迁移, 2D-3D电池器件显示出明显增强的长期稳定性, 在200 h内一直保持初始转换效率, 甚至在500 h后仍能保持其初始转化效率的90%.

  